



Spatial distribution of oxygen chemical potential under potential gradients and performance of solid oxide fuel cells with $\text{Ce}_{0.9}\text{Gd}_{0.1}\text{O}_{2-\delta}$ electrolyte



In-Ho Kim^a, Bhupendra Singh^b, Yeon Naungung^a, Sun-Ju Song^{a,*}

^a Ionics Lab, School of Materials Science and Engineering, Chonnam National University, 77, Yongbong-ro, Buk-gu, Gwang-Ju 500-757, Republic of Korea

^b CSIR-Advanced Materials and Processes Research Institute (AMPRI), Hoshangabad Road, Bhopal 462026, India

ARTICLE INFO

Keywords:

Gadolinium doped ceria
Electrolyte
Oxygen chemical potential
Partial conductivity

ABSTRACT

In this work, maximum power density as a function of electrolyte thickness of a solid oxide fuel cell (SOFC) with $\text{Ce}_{0.9}\text{Gd}_{0.1}\text{O}_{2-\delta}$ (GDC10) electrolyte was calculated by integrating partial conductivities of charge carriers under various DC bias conditions at a fixed oxygen chemical potential gradient at both sides of the electrolyte. Partial conductivities as a function of temperature and oxygen partial pressure (P_{O_2}) were calculated using Hebb-Wagner polarization method and spatial distribution of P_{O_2} across the electrolyte was calculated based on Choudhury and Patterson's model [1] by considering reversible electrode conditions. At terminal voltages corresponding to SOFC and electrolysis cell operation modes, the oxygen chemical potential gradient at a electronic-stoichiometric point became maximum and minimum to compensate the contribution from electrochemical potential gradient of electron. The current-voltage characteristics in different fuel cell conditions with temperature and thickness dependence were calculated with cathodic and anodic P_{O_2} of 0.21 and 10^{-22} atm, respectively. The theoretical maximum power density increased from $1.26 \text{ W}\cdot\text{cm}^{-2}$ at 500°C to $7.39 \text{ W}\cdot\text{cm}^{-2}$ at 700°C . Similarly, at 500°C , power density increased two fold on reducing electrolyte thickness from $20 \mu\text{m}$ to $10 \mu\text{m}$. The implications of these results on the development of GDC10 based SOFC systems was discussed.

1. Introduction

Alivalent cation doped ceria has been widely used as solid electrolyte in electrochemical devices at intermediate temperatures and has been preferred over conventional zirconia oxide based electrolytes in several areas such as higher ionic conduction at low temperature [2], and has shown better chemical compatibility with common fuel cell cathodes and separation membranes [3–5]. It, however, is a mixed conductor and undergoes large departures from stoichiometry at elevated temperatures and in reducing atmosphere with conduction occurring predominantly by oxygen vacancies or by electrons depending on the departure from stoichiometry [6, 7]. Investigations on the elastic properties of both pure ceria and gadolinia doped ceria (GDC) found that these materials show significant elastic softening as the oxygen partial pressure decreased, i.e., as ceria becomes more hypo-stoichiometric and GDC contains more oxygen vacancies [8]. A detailed evaluation of the effects of such behaviors of GDC in SOFC applications has been made by using finite difference model [9, 10].

The occurrence of electronic conductivity in GDC is expected to enhance catalytic and electrochemical activities for fuel oxidation and oxygen reduction for SOFCs and it was observed that the performance

of SOFC electrodes was improved by adding GDC [11, 12], however, a decrease in open circuit voltage (OCV) was observed due to the current leakage [13]. Wachsman and Duncan have suggested that OCV of ceria based SOFC is dependent upon the electrolyte thickness [14]. In fuel cell operating conditions, the partial electronic conduction in GDC induces oxygen-permeation across the electrolyte, which in turn leads to changes in P_{O_2} and results in an increase in effective P_{O_2} at anode and a decrease in effective P_{O_2} at cathode [15]. Although a reduced electrolyte thickness reduces the OCV value, it increases power density by reducing ohmic and polarization resistances [16, 17].

Though, in case of pure electrolyte, the electrical conductivity may not be altered by the variation of the spatial distribution of chemical potential across the specimen, because GDC electrolyte is often mentioned as a mixed ionic-electronic conductor (MIEC) under highly reducing conditions, the non-linear I–V characteristics under a chemical potential gradient may be observed. Therefore, operational performance of SOFC using GDC electrolyte should be understood by considering partial currents of each charge species, which is determined by the terminal voltage of the cell. In this work, the influence of mixed conductivity in GDC10 electrolyte with respect to its thickness, on the current-voltage characteristics, efficiency, and performance was

* Corresponding author at: School of Materials Science and Engineering, Chonnam National University, 77 Yongbong-ro, Buk-gu, Gwang-Ju 500-757, Republic of Korea.
E-mail address: song@chonnam.ac.kr (S.-J. Song).

analyzed by calculating the spatial distribution of oxygen partial pressure across the GDC electrolyte in an oxygen chemical potential gradient as a function of various terminal voltages, based on the partial conductivities measured from Hebb-Wagner polarization measurements. The spatial distribution of oxygen partial pressure across the electrolyte was calculated based on Choudhury and Patterson's work [1, 18] by considering zero electrode polarization. By integrating partial conductivities of charge carriers under various DC bias conditions at a fixed oxygen chemical potential gradient at both sides of the electrolyte, the maximum power density of SOFC that can be obtained from a given electrolyte thickness was reported.

2. Experimental

10 mol% Gd^{3+} -doped ceria commercial powder (GDC10, HP grade, Fuel cell materials) was molded into disc and bar shaped specimens. The specimens were further compacted by cold isostatic pressing (CIP) under 150 MPa. The CIPed specimens were sintered at 1400 °C for 10 h in air. A ~1.5 mm thick disc was cut from the sintered disc specimen for the Hebb-Wagner polarization experiment. Similarly, a $1.8 \times 1.8 \times 11 \text{ mm}^3$ bar was cut from the sintered bar specimen for electrical conductivity measurements. The surfaces of the cut specimens were polished by emery paper to minimize the surface roughness. A part of the remaining sintered specimen was ground to powder for X-ray diffraction analysis using an X-ray diffractometer (Rigaku high resolution powder X-ray diffractometer) equipped with a $Cu-K\alpha$ radiation source (1.5406 Å) and operating at 40 kV and 30 mA at a scan rate of 2°/min between scanning angles (2θ) of 10–80°. The XRD pattern was fitted by Rietveld refinement method and the theoretical density of GDC was calculated by lattice parameter obtained from the refinement result. The microstructure of the fractured section of the sintered specimen was analyzed using a field-emission scanning electron microscope (INSPECT 50 FEI). The experimental density of the sintered specimen was measured by Archimedes method.

A Hebb-Wagner polarization cell was applied to measure the I–V characteristics of GDC10 under polarization by applying a voltage between the positive reversible electrode (Pt mesh) and negative ion-blocking electrode (Pt foil) [19]. The configuration of the Hebb-Wagner polarization cell in four-probe setup is given in details elsewhere [20]. The currents were applied and the saturation voltages were measured, while carefully keeping it well below the phase decomposition voltage. The electrical conductivity was measured by DC 4-probe method using the bar-shaped specimen, a digital multimeter (Keithley 2700) and a current source (Keithley 6220) at various temperatures in $700 \leq (T/^\circ\text{C}) \leq 1000$ range and oxygen partial pressures in $0.21 \leq (P_{O_2}/\text{atm}) \leq 10^{-23}$ range.

3. Results and discussion

Fig. 1(a) shows XRD pattern of the GDC10 powder obtained from the crushed sintered specimen. The pattern shows reflections which can be assigned to cubic ceria phase. The lattice parameter obtained from the Rietveld refinement was $a = 5.41 \text{ \AA}$. Fig. 1(b) shows the SEM image of the fractured section of the sintered GDC10 specimen. The specimen was highly dense with well-developed grains. The relative density was 99.4% and the average grain size was 70 nm.

Hebb-Wagner polarization method has been widely used for the estimation of partial electronic conductivities in doped ceria-based systems [21–26]. In the present work, the electrochemical cell used for the Hebb-Wagner polarization experiment is schematically shown in Fig. 2(a). Typical temporal variation of the voltage U across the Hebb-Wagner polarization cell when constant currents of 3, 5, 10, 20 μA are switched on and off in turns at 900 °C with the reference oxygen activity in air is shown in Fig. 2(b). When the current was applied, an initial rapid increase followed by convergence to the steady-state in voltage was observed and no voltage difference was confirmed by noting the

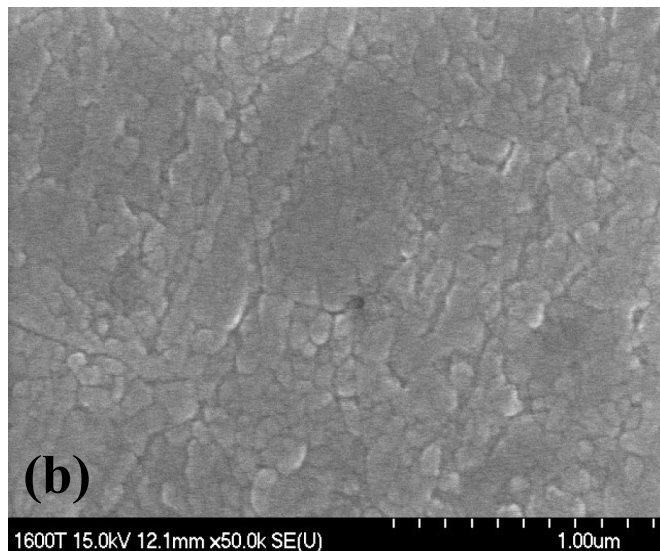
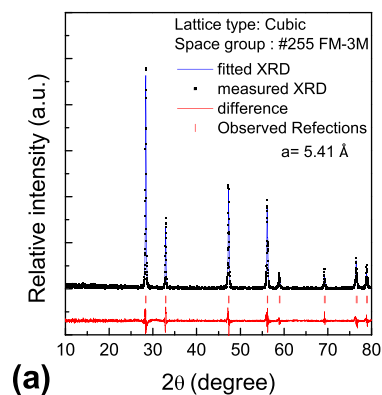


Fig. 1. (a) XRD pattern of the GDC10 powder obtained from the crushed sintered specimen and (b) SEM image of the fractured section of the sintered GDC10 specimen.

voltage back to the original state while turning-off the current. The experimental data collected for the polarization experiment at 900 °C are shown in Fig. 3(a). The potential pitfalls with Hebb-Wagner polarization cell for determining electronic conductivity are possible leak or oxygen exchange through the sealed lateral boundary and electrode overpotentials [19, 20]. To confirm the sealing issue causing electrochemical reaction at the blocking electrode and side of specimen, the typical steady-state value of I–V characteristics collected in air were shown in Fig. 3(a) and congruent results were observed.

Within the electrolytic domain, the partial conductivities of electrons and holes in GDC obey 1/4 and $-1/4$ power dependencies on the oxygen partial pressure [19]:

$$\sigma_e = \sigma_n^* \left(\frac{pO_2}{pO_2^*} \right)^{-1/4} + \sigma_p^* \left(\frac{pO_2}{pO_2^*} \right)^{1/4} \quad (1)$$

where σ_n^* and σ_p^* are the electron and hole conductivity at the reference oxygen partial pressure. Whereas, total electronic currents through the polarization cell can be described as:

$$I_e = \frac{ART}{LF} \left[\sigma_n^* \left\{ \exp\left(\frac{EF}{RT}\right) - 1 \right\} + \sigma_p^* \left\{ 1 - \exp\left(-\frac{EF}{RT}\right) \right\} \right] \quad (2)$$

Details for derivation of Eq. (2) can be found in literature [20]. The solid line in Fig. 3(a) represented the best fitted to Eq. (2).

The partial electron and hole conductivity may be represented as functions of temperature and oxygen partial pressure as:

Download English Version:

<https://daneshyari.com/en/article/7744193>

Download Persian Version:

<https://daneshyari.com/article/7744193>

[Daneshyari.com](https://daneshyari.com)